MLA

ELECTROKINETIC-POTENTIAL FLUCTUATIONS GENERATED BY JET IMPINGEMENT

by

Dr. L. Duckstein, Junior Civil Engineer
Civil Engineering Department
Colorado State University
Fort Collins, Colorado

and

Dr. J. E. Cermak, Professor of Civil Engineering
and Engineering Mechanics
Civil Engineering Department
Colorado State University
Fort Collins, Colorado

Paper to be Submitted to the
International Journal of Heat and Mass Transfer

June 1962 CER62LD40

ABSTRACT

Electrokinetic-potential fluctuations produced by a two-dimensional submerged water jet impinging on a plate have been measured. The potential fluctuations are postulated to be linearly related to the three velocity-fluctuation components u'_x , u'_y , u'_z . In the particular case when $u'_x > u'_y > u'_z$, the potential fluctuations are approximately proportional to the longitudinal-velocity fluctuations u'_x .

Normalized frequency distributions of potential-fluctuation measurements agree with velocity-fluctuation data taken by Klebanoff and Laufer with a hot-wire anemometer at a dimensionless distance $y/\delta \simeq 10^{-3}$ from the wall. The hypotheses made concerning the relationship between potential and velocity fluctuations give a possible explanation of the change in the shape of the potential-fluctuation spectrum with the flow velocity and the electrical conductivity of the water.

LIST OF SYMBOLS

Symbol	Definition	Dimension*
d	double layer thickness	m
e	base of natural logarithm	n.d.
e_o	charge of the electron, coulombs	sa
e_r	RMS value of the net amplified signal	$m^2ks^{-3}a^{-1}$
e_{ro}	value of e_r at the stagnation point	- - -
e_w	net voltage read on the wave analyzer	- - -
f	frequency	s^{-1}
f_m	maximum frequency of velocity fluctuation considered	s^{-1}
g	acceleration of gravity	ms^{-2}
k	Boltzman constant, 1.38×10^{-23} joules/deg.	$m^2ks^{-3}t^{-1}$
k_1	wave number in data of others	m^{-1}
ℓ	characteristic length of flow near the wall	m
n	wave number	m^{-1}
n_o	number of ions per unit volume in the bulk of the liquid	m^{-3}
p_o	stagnation pressure	$m^{-1}ks^{-2}$
q	surface charge density, coul/m^2	$m^{-2}sa$
u	velocity	ms^{-1}
u_x, u_y, u_z	velocity components along ox, oy, oz	ms^{-1}
x	longitudinal coordinate	m
x_2	origin of established mean flow in x direction	m
y	vertical coordinate	m
z	transversal coordinate	m

* The dimension symbols are: m - meter, k - kilogram, s - second, a - ampere, t - temperature, n.d. - no dimension.

LIST OF SYMBOLS (Continued)

Symbol	Definition	Dimension
B_o	band width	s^{-1}
C	constant (Eq. 4)	n.d.
E_u	normalized spectral distribution of u'_x	m or s
$E'_{\Delta\psi}(f)$	spectral distribution of the potential-difference fluctuations, $(mV)^2$ sec.	$m^4 k^2 s^{-5} a^{-2}$
$E'_{\Delta\psi}(n)$	spectral distribution of the potential-difference fluctuations, $(mV)^2$ cm.	$m^5 k^2 s^{-6} a^{-2}$
$E_{n\Delta\psi}$	normalized value of $E'_{\Delta\psi}(f)$ or $E'_{\Delta\psi}(n)$	m or s
H	hydrostatic head	m
L	orifice-plate distance	m
T	absolute temperature, degrees Kelvin	t
U	velocity at the slot $(2gH)^{1/2}$	ms^{-1}
δ	boundary-layer thickness	m
ϵ	permittivity of water, farads/m	$m^{-3} k^{-1} s^4 a^2$
ν	kinematic viscosity of water	$m^2 s^{-1}$
ρ	mass density of water	$m^{-3} k$
ρ_c	electric charge density, coul/m^3	$m^{-3} sa$
σ	conductivity	$m^{-3} k^{-1} s^3 a$
τ	relaxation time, $\epsilon\sigma^{-1}$	s
τ_w	shear at the wall	$m^{-1} ks^{-2}$
ψ	electrical potential	$m^2 ks^{-3} a^{-1}$
$\nabla\psi$	electrical potential-difference	$m^2 ks^{-3} a^{-1}$
∇	differential operator	- - -
∇^2	laplacian	- - -
$\underline{(\ )}$	vector	- - -
$(\ )'$	time-fluctuating component	- - -
$\overline{(\ )}$	time-mean value	- - -

REVIEW OF THE PROBLEM

Introduction. In general, an electrical double layer arises at the interphase boundary between a liquid and a solid; it is composed of ions of a certain sign attached to the solid wall and of a diffuse layer of the opposite sign, which can move with the liquid. This double layer is a few hundred angstroms thick. When the charge distribution in the double layer is disturbed by velocity fluctuations, potential-difference fluctuations arise, and may be picked up by electrodes along the wall.

The present investigation was aimed at relating the potential fluctuations to the velocity field, close to the wall where existing turbulence-measurement techniques, such as the hot-wire anemometer, become very difficult to use. A two-dimensional jet impinging on a perpendicular plate was the turbulent flow field chosen for this study. The high level of turbulence of such a jet flow produced a readily measured potential fluctuation. The results found in pipe flow by Binder [1] were extended to a non-uniform flow case.

Deviation of the Fundamental Equations. In addition to the usual assumptions made in the deviation of the D.C. streaming potential equation [2], the following assumptions suggested by experimental results [1,3] were used:

(1) the diffuse-layer thickness d is approximately the same in a turbulent flow case as is the static case, that is, $d \sim 5 \times 10^{-6}$ cm for the present experimental conditions;

(2) at any instant the time-fluctuating component ψ' of the potential ψ satisfies the inequalities

$$|\psi'| < |\overline{\psi}| \quad \text{and} \quad \left|\frac{e_o \psi'}{kT}\right| << 1. \tag{1}$$

In the static case, the charge distribution in a mono-monovalent electrolyte close to a wall is written as [4,5]

$$\rho_c = -2\, n_o e_o \sinh\left(\frac{e_o\psi}{kT}\right) . \tag{2}$$

The potential distribution is obtained by integration of Poisson's equation where ρ_c is given by Eq. 2:

$$\frac{d^2\psi}{dy^2} = \frac{-\rho_c}{\epsilon} = \frac{2\, n_o e_o}{\epsilon} \sinh\left(\frac{e_o\psi}{kT}\right) . \tag{3}$$

The result is:

$$\psi = \frac{2kT}{e_o} \operatorname{Ln}\left(\frac{1 + Ce^{-y/d}}{1 - Ce^{-y/d}}\right) . \tag{4}$$

In this equation, C can be expressed as a function of the surface charge density of the wall q , and d is the thickness of the double layer:

$$d = \left(\frac{\epsilon\, kT}{2\, n_o e_o^{\,2}}\right)^{1/2} . \tag{5}$$

When a small disturbance is introduced into the charge distribution defined by Eq. 2 [6], the relation between the charge and the potential fluctuations can be written, using condition (1) as:

$$\rho'_c = \left\{\frac{2\, n_o e_o^{\,2}}{kT} \cosh\left(\frac{e_o\bar{\psi}}{kT}\right)\right\} \psi' . \tag{6}$$

With Eqs. 2 and 5, Eq. 6 yields:

$$\rho'_c = \frac{\epsilon}{d^2}\left\{1 + \left(\frac{\bar{\rho}_c}{2\, n_o e_o}\right)^2\right\}^{1/2} \psi' . \tag{7}$$

The approximate relation between the velocity and potential fluctuations can be postulated as [1]:

$$\sigma \nabla^2 \psi' = \underline{u}' \cdot \underline{\nabla} \bar{\rho}_c \quad . \tag{8}$$

Combining Eqs. 7, 8, and Poisson's equation for fluctuating components $\nabla^2 \psi' = -\frac{\bar{\rho}_c}{\epsilon}$ and using assumption (1), one obtains the relation:

$$\underline{u}' \cdot \underline{\nabla} \bar{\rho}_c = \frac{\sigma}{d^2} \left[1 + \left(\frac{\bar{\rho}_c}{2 n_o e_o} \right)^2 \right]^{1/2} \psi' \quad . \tag{9}$$

The physical meaning of this equation is that the potential fluctuations are produced by the fluctuating component $\underline{u}'$ along the mean charge-density gradient. A way to simplify Eq. 9 might consist in considering that $\bar{\rho}_c$ is a function of y only. In the left-hand member, one would be left with one term only, $u'_y \frac{\partial \bar{\rho}_c}{\partial y}$, thus ψ' would be caused by vertical-velocity components. This is apparently contradicted by the experimental results of Chuang [7]

On the other hand, Eq. 9 may yield an acceptable result if it is assumed that the electrode introduces a non-homogeneity into the mean-charge distribution and, further that this non-homogeneity creates a mean-charge distribution gradient in the x and z direction of the same order of magnitude as $\frac{\partial \bar{\rho}_c}{\partial y}$. Under these assumptions, Eq. 9 can be approximately written as

$$\left(u'_x + u'_z \right) \frac{\partial \bar{\rho}_c}{\partial x} = \frac{\sigma}{d^2} \left\{ 1 + \left(\frac{\rho_c}{2 n_o e_o} \right)^2 \right\}^{1\,2} \psi' , \tag{10}$$

since $\frac{\partial \bar{\rho}_c}{\partial x} \backsimeq \frac{\partial \bar{\rho}_c}{\partial y} \backsimeq \frac{\partial \bar{\rho}_c}{\partial z}$ by hypothesis, and $u'_y < u'_x$ and u'_z near the

wall for a flat plate boundary-layer flow. The latter approximation is taken from the experimental results of Klebanoff [8], Laufer [9], and others in turbulent boundary-layer flow; that is, $u'_y < u'_z < u'_x$ close to the boundary. Assuming that

$$\frac{\partial \bar{\rho}_c}{\partial x} \simeq \frac{\bar{\rho}_c}{\ell} \quad . \tag{11}$$

where ℓ is the small but finite length over which the discontinuity of $\bar{\rho}_c$ occurs, Eq. 10 may be roughly approximated as

$$\psi' \simeq \frac{d^2 \bar{\rho}_c}{\sigma \ell} \left\{ 1 + \left(\frac{\bar{\rho}_c}{2 n_o e_o} \right)^2 \right\}^{-1/2} u'_x \quad . \tag{12}$$

A physical representation of Eqs. 10 and 12 may be given as follows: the potential fluctuations ψ' are caused by longitudinal-velocity fluctuations u'_x disturbing the charge distribution at a distance of order d from the boundary between the electrode and the plate.

Application to the Present Investigation. From Eq. 12, it follows that the RMS value of the amplified signal e_r, which is proportional to $\sqrt{\overline{\psi'^2}}$, varies as $\sqrt{\overline{u'^2_x}}$. According to Klebanoff [8], Laufer [9], and Hinze [10], the RMS value of the velocity fluctuations $\sqrt{\overline{u'^2_x}}$ is proportional to the local-mean velocity $\bar{u}_x$ very close to the wall. On the other hand, the local mean velocity varies as the wall shear. Wall jet measurements by Myers and others [11], in agreement with data taken by previous investigators, show that the wall shear is inversely proportional to the longitudinal distance x (see definition sketch in Fig. 1, which includes the symbol key for all subsequent figures).

As the plane jet impinging upon a plate is similar to a wall jet for $x > x_2$, it follows that e_r should vary as x^{-1} for $x > x_2$.

For $x < x_2$, dimensional considerations [6] show that either one of the parameters:

$$\frac{e_r^2 \sigma}{\rho U^4} f_m \, , \quad \frac{e_r^2 \sigma}{\rho U^4 \tau} \, ,$$

should be a constant of the flow; f_m represents maximum frequency of potential fluctuation considered and τ is the relaxation time of the water. The distance x_2 must be determined by experiment.

EQUIPMENT AND PROCEDURE

The Flow System. A schematic of the constant-head system with overflow at various heights H, built for this investigation, is shown in Fig. 2. Only materials which do not contaminate distilled water such as lucite, brass, and platinum, were used. The elevation of the diffuser could be changed so that the flow may be undisturbed just before the outlet. The orifice itself (0.1 x 2.65 cm) was brass; the jet impinged upon a lucite plate fixed in a plexiglass tank, which could be moved in the x and y direction. The water in the tank was kept at a constant level; it was then recirculated through a weir box and polyethylene bottles, by means of an ECO "teflon" and stainless steel pump (type 22U2 Allchem). The conductivity of the equilibrium water introduced into the system stabilized itself around 4.5 micromhos/cm after several days.

The Electrical System. In order to eliminate electrical pick-up, especially the 60c/s one, a grounded enclosure in sheet metal was built around the experimental set-up (Fig. 3). The pump was located outside of this

shielding and two grounded brass rings were incorporated into the plastic tubing, downstream and upstream of the pump, respectively.

The results presented here were taken with .081 cm diameter platinum electrodes, placed and connected as indicated in Figs. 1 and 3, and sealed by a rubber adhesive. Data taken with .081 cm diameter copper wire showed that dimensionless ratios, such as normalized spectra, were not affected by the material of the electrodes, as hypothesized by Binder [1]. Platinum was used in order to obtain reliable results when the conductivity of the water was increased.

From the electrodes, the signal was fed into a Tektronix type 122 low-level preamplifier. The 60 c/s pick-up was reduced to a negligible quantity by grounding the brass orifice, the reference electrode and the cable shieldings at one point only, thus eliminating ground currents. The amplification factor of the preamplifier was 1200 and input impedance was 10^7 ohms. Since the impedance between two electrodes was normally less than 10^5 ohms, no appreciable distortion of the signal was to be expected. The output of the preamplifier was fed into a wave analyzer (Hewlett-Packard, Model 300A) or a sinusoidal RMS meter (Hewlett-Packard, Model 400H). An oscilloscope (Tektronix type 502) was always connected in parallel with either the wave analyzer or the RMS meter, so that the signal could be observed.

The wave analyzer had a constant band width, the value of which was $B_o = 14.55$ c/s, if the definition given for the band width by Klebanoff [8] B_o is the rectangular band width having the same area as the actual band shape, was adopted. The difference between the true RMS value of the signal, found by graphical integration of the frequency spectral distribution, and the value given by the RMS meter, was about 5 percent.

Procedure. The electrodes were submerged for several hours in water before each run. When a steady flow was obtained at the desired head (Figs. 1,2), the instruments were switched on and allowed to warm up for half

an hour. Measurements were then taken, at least twice; finally, the total noise caused by the pump, diffuser, pick-up and instruments was measured by covering the electrodes with a plexiglass plate. The value of the noise found by this method did not differ appreciably from the value measured in still water. The noise seemed thus to be principally caused by the instruments.

When the influence of the conductivity on the signal was studied, constant amounts of saturated KCl solution were added to the water at given intervals of time. Data were taken half an hour after the conductivity was found to remain constant, that is, about every two hours. After the run, the system was flushed several times with distilled water.

RESULTS AND DISCUSSION

Reproducibility of Data. The signal amplitude taken with a given pair of electrodes was reproducible within experimental error for a few days. Then, as noticed by most investigators, the signal amplitude changed progressively, presumably because the electrical double layer was modified. The conductivity seemed to play an important role in this drift. The total error in taking data, which included random error due to fluctuations of the instruments indicator during a given experiment and systematic error, due to personal factors or day-to-day changes, was estimated at less than 10 percent.

The results found for the RMS value of the signal, taken with one electrode connected to the amplifier and another electrode grounded, are presented first. The spectral density distribution of the potential fluctuations are presented next, and compared to velocity-fluctuation data.

Root-Mean-Square of the Potential Fluctuation. The RMS value of the signal e_{r_ρ} at the stagnation point is proportional to the stagnation pressure

p_o (Fig. 4). The variation of the ratio $\frac{e_r}{e_{ro}}$ with the longitudinal distance x is shown in Fig. 5: $e_r = e_{ro}$ for $x < .35$ cm and $\frac{e_r}{e_{ro}} = \frac{.35}{x}$ for $x > .35$ cm. This variation is independent of the location of the grounded electrode. These results seem to confirm the assumptions made above, which let to a proportionality of e_r^2 and $\overline{u'^2_x}$, and described the expected variation of $\overline{u_x}$ with p_o (or U) and x from wall jet measurements made by others. In particular, the value x_2 mentioned at the end of the section "Review of the Problem" may be taken as .35 cm for the configuration used. For a study of the influence of the conductivity σ upon the value of e_r, a distinction had to be made between continuous runs and separate runs. Several hours were necessary for the double layer to reach a new equilibrium after new ions had been introduced into the water. The variation of e_r^2 with σ for separate runs, which represents the most useful case, is shown in Fig. 6 e_r^2 varies approximately as σ^{-1} in the range of conductivities considered.

The dimensionless parameter $\frac{e_r^2 \sigma}{\rho U^4} f_m$, proposed earlier, appears as a possible constant of the flow; one should note that by definition, p_o is proportional to ρU^2 for a given value of L (Fig. 1).

Spectral Distribution. If e_w is the net quantity read on the wave analyzer, the frequency spectral distribution of the amplified potential-difference fluctuations is by definition:

$$E'_{\Delta\psi}(f) = \frac{e_w^2}{B_o} \text{ (millivolts)}^2 \text{ sec.} \qquad (13)$$

It is convenient to define a wave number spectrum as

$$E'_{\Delta\psi}(n) = \frac{e_w^2}{B_o} \frac{\overline{U}}{2\pi} \text{ (millivolts)}^2 \text{ cm},$$

$$\text{with } n = \frac{2\pi f}{\overline{U}} = \frac{2\pi f}{(2gH)^{1/2}} \text{ cm} . \tag{14}$$

Finally, the normalized spectra are obtained by dividing $E'_{\Delta\psi}(f)$ and $E'_{\Delta\psi}(n)$ by the mean-square value of the signal e_r^2.

The change of the shape of the normalized spectrum at the stagnation point as the head is varied is shown in Figs. 7 and 8. The frequency power spectrum rotates clockwise, which means that the relative amount of low-frequency fluctuation increases and the relative amount of high-frequency fluctuation decreases, as the head is decreased. The wave number spectrum is almost the same for all heads. Similarly, the curve $E_{n\Delta\psi}(f)$ rotates counter-clockwise when the conductivity σ is increased, as shown in Fig. 9. The relative amount of high-frequency energy seems thus to increase as H or σ are increased.

According to the physical representation of the phenomenon discussed above, (see Eq. 12), the potential-fluctuation measurements represent the longitudinal-velocity fluctuation at a distance of order d from the electrode-plate boundary. The value of d defined by Eq. 5, is about 5×10^{-6} cm when the conductivity is 5 micromhos/cm [1]. If the boundary-layer thickness is computed from the formula for a smooth flat plate in turbulent flow [12]:

$$\delta(x) = .37\, x^{4/5} \left(\frac{\nu}{U_\infty} \right)^{1/5} , \tag{15}$$

one finds $\delta \simeq 10^{-2}$ cm for the conditions corresponding to Fig. 10: $x = .2$ cm , $p_o \simeq 100$ cm of water for $H = 413$ cm. With these conditions the calculated dimensionless distance from the wall $\frac{d}{\delta}$ is approximately

5×10^{-4}. The normalized frequency spectra of potential fluctuations corresponding to that value of $\frac{d}{\delta}$ agree well with velocity-fluctuation spectra taken by Klebanoff [8] at $\frac{y}{\delta} = 1.1 \times 10^{-3}$, as can be seen in Fig. 10. A similar comparison is made between wave number spectra in Fig. 11. The data seem to fit an n^{-7} variation at high wave numbers, which would confirm the assumptions of Tchen [13] that the high-frequency velocity fluctuations are not affected by shear.

At any rate, the spectral distribution curves always shift in a counter-clockwise direction as the calculated value of $\frac{d}{\delta}$ or experimental value of $\frac{y}{\delta}$ is decreased. Calculated values of $\frac{d}{\delta}$ as a function of an initial value $\frac{d_o}{\delta_o}$ are shown in Fig. 9, where δ stays constant $\left(\delta = \delta_o\right)$ and d changes according to Eq. 5, that is, $d \simeq \sigma^{-1/2}$, approximately. Similar computations are shown in Fig. 12, but here d stays constant and δ varies according to Eq. 15; the second moment of the spectral distribution emphasizes the change in the shape of the spectrum at medium frequencies. It can be seen on all three figures 10, 11, 12, that the spectral distribution curves always shift in a counter-clockwisedirection as the calculated value of $\frac{d}{\delta}$ or the experimental value of $\frac{y}{\delta}$ is decreased; in other words, the proportion of high-frequency fluctuations seems to increase as one approaches the wall.

If further experiments would confirm the assumptions and results presented in this paper, the electrokinetic method could then be used to study turbulent shear flows very close to the wall. The dimensionless distance from the wall $\frac{d}{\delta}$, at which the velocity fluctuations occur according to the hypothesis, could be changed at will by acting either on the conductivity which changes d, or on the velocity which changes δ, depending on the case considered.

CONCLUSIONS

The conclusions derived from this experimental study of the electro-kinetic-potential fluctuations created by jet impingement are:

(1) The root-mean-square value of the amplified potential-fluctuation signal at the wall is proportional to the stagnation pressure on the plate. As the stagnation pressure is increased, the normalized frequency spectrum shifts counter-clockwise, which means that the relative amount of high-frequency energy increases with the hydrostatic head. The normalized wave number spectrum, where the wave number is defined as $2\pi f(2gH)^{-1/2}$, remains nearly invariant with the stagnation pressure.

(2) Along the longitudinal axis ox, the RMS value of the signal remains approximately constant near the stagnation point; then it decreases as x^{-1}.

(3) The value of the electrical conductivity of the water has a definite influence on the signal. The RMS value of the signal varies approximately as the square-root of the conductivity for low and medium conductivities. The normalized frequency spectrum shifts in the same manner, when the conductivity is increased, as when the stagnation pressure is increased.

(4) The normalized spectrum of the potential fluctuations compares well with normalized spectrum of longitudinal-velocity fluctuations, measured by Klebanoff with a hot-wire anemometer at a dimensionless distance $\frac{y}{\delta} \simeq 10^{-3}$ from the wall, in a two-dimensional turbulent boundary-layer flow. The extimated value of the dimensionless distance from the wall at which the velocity fluctuations would be measured, according to the hypotheses made in this study, is of the same order of magnitude as $\frac{y}{\delta}$.

(5) No directional sensitivity of a pair of electrodes, placed 0.4 cm apart, can be detected with one of the electrodes permanently grounded.

ACKNOWLEDGEMENT

Financial assistance for this study through a National Science Foundation grant, is gratefully acknowledged.

REFERENCES

[1] G. J. Binder, Electrokinetic-Potential Fluctuations Produced by Turbulence at a Solid-Liquid Interface. Doctoral Dissertation, Colorado State University, Fort Collins, 1960. 121 p.

[2] L. A. Wood, An Analysis of the Streaming Potential Method of Measuring the Potential at the Interface Between Solids and Liquids. Journal of the American Chemical Society 68, pp. 432-434, 1946.

[3] A. A. Boumans, Streaming Currents in Turbulent Flows and Metal Capillaries. Physica 23, (11), 1007-1055. November 1957.

[4] S. Glasstone, Textbook of Physical Chemistry, (Second Edition), Ch. 14, D. Van Nostrand, New York, 1958.

[5] S. M. Neale, The Electrical Double Layer, the Electrokinetic Potential and the Streaming Current. Transactions of the Faraday Society, 42, pp. 473-478, 1946.

[6] L. Duckstein, Electrokinetic-Potential Fluctuations Generated by Jet Impingement at a Solid-Liquid Interface, Doctoral Dissertation, Colorado State University, Fort Collins. 1962. 110 p.

[7] H. Chuang, Electrokinetic-Potential Fluctuations Produced by Turbulence in Fully Developed Pipe Flow. Doctoral Dissertation, Colorado State University, Fort Collins. 1962. 111 p.

[8] P. S. Klebanoff, Characteristics of Turbulence in a Boundary Layer with Zero Pressure Gradient. U. S. National Advisory Committee for Aeronautics, Report 1247, 1955. 19 p.

[9] J. Laufer, Investigation of Turbulent Flow in a Two-Dimensional Channel. U. S. National Advisory Committee for Aeronautics, Report 1053, 1951. 20 p.

[10] J. O. Hinze, Turbulence, (First Edition), Ch. 7, McGraw-Hill New York. 1959.

REFERENCES Continued

[11] G. E. Myers, J. J. Schauer, and R. H. Eustis, The Plane Turbulent Wall Jet. Part I. Jet Development and Friction Factors. Technical Report No. 1, Department of Mechanical Engineering, Stanford University, Stanford, California, 1961. 33 p.

[12] H. Schlichting, Boundary Layer Theory, (Fourth Edition), p. 537, McGraw-Hill, New York, 1960.

[13] C. M. Tchen, On the Spectrum of Energy in Turbulent Shear Flow. U. S. National Bureau of Standards, Journal of Research, Research Paper 2388, 50, (1), pp 51-62. January 1953.

FIGURES

Figure No.	Title
1.	Definition Sketch
2.	Flow System
3.	Electrical System
4.	Variation of Amplified Potential-Fluctuations with Stagnation Pressure
5.	Variation of Amplified Potential-Fluctuations at the Wall as a Function of Distance from Stagnation Point.
6.	Mean-Square of Amplified Wall Potential-Fluctuations with Electrical Conductivity of the Water
7.	Frequency Spectrum at the Stagnation Point
8.	Wave Number Spectrum at the Stagnation Point
9.	Variation of the Frequency Spectrum with the Electrical Conductivity of the Water
10.	Normalized Spectra for Potential and Velocity Fluctuations
11.	Normalized Spectra for Potential and Velocity Fluctuations
12.	Second Moment of Spectral Distribution

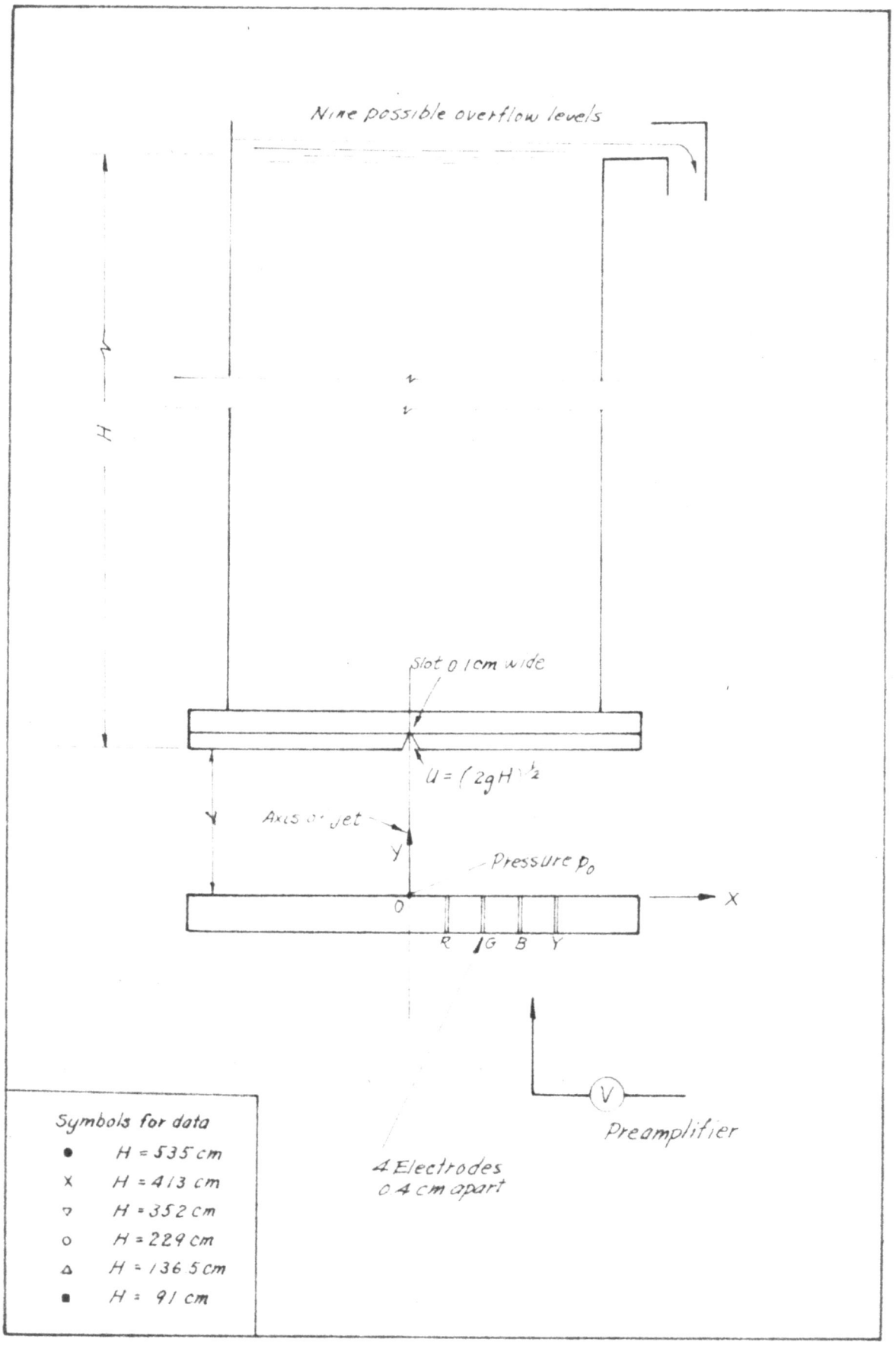

Fig. 1 Definition Sketch

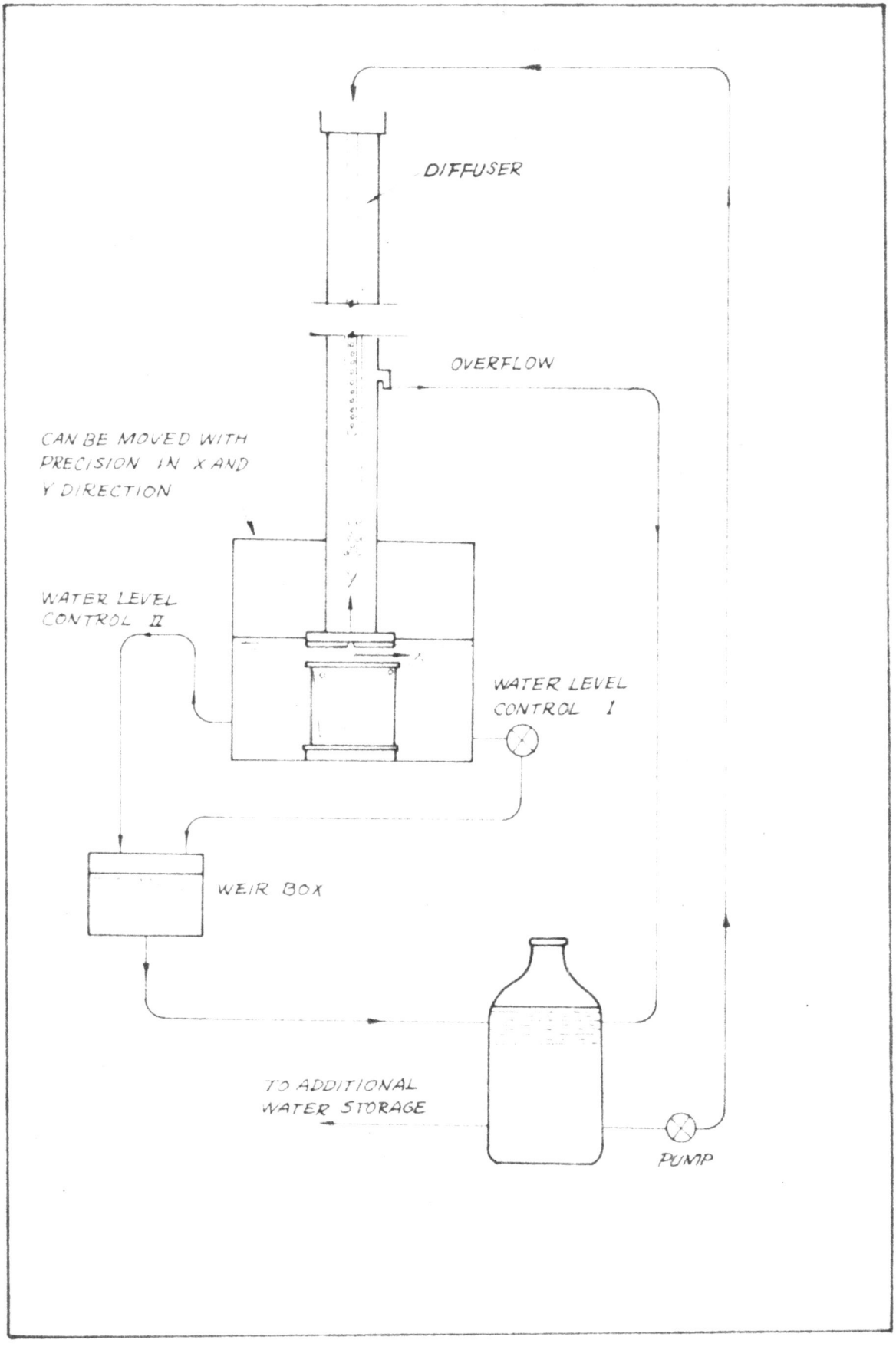

Fig. 2 Flow System

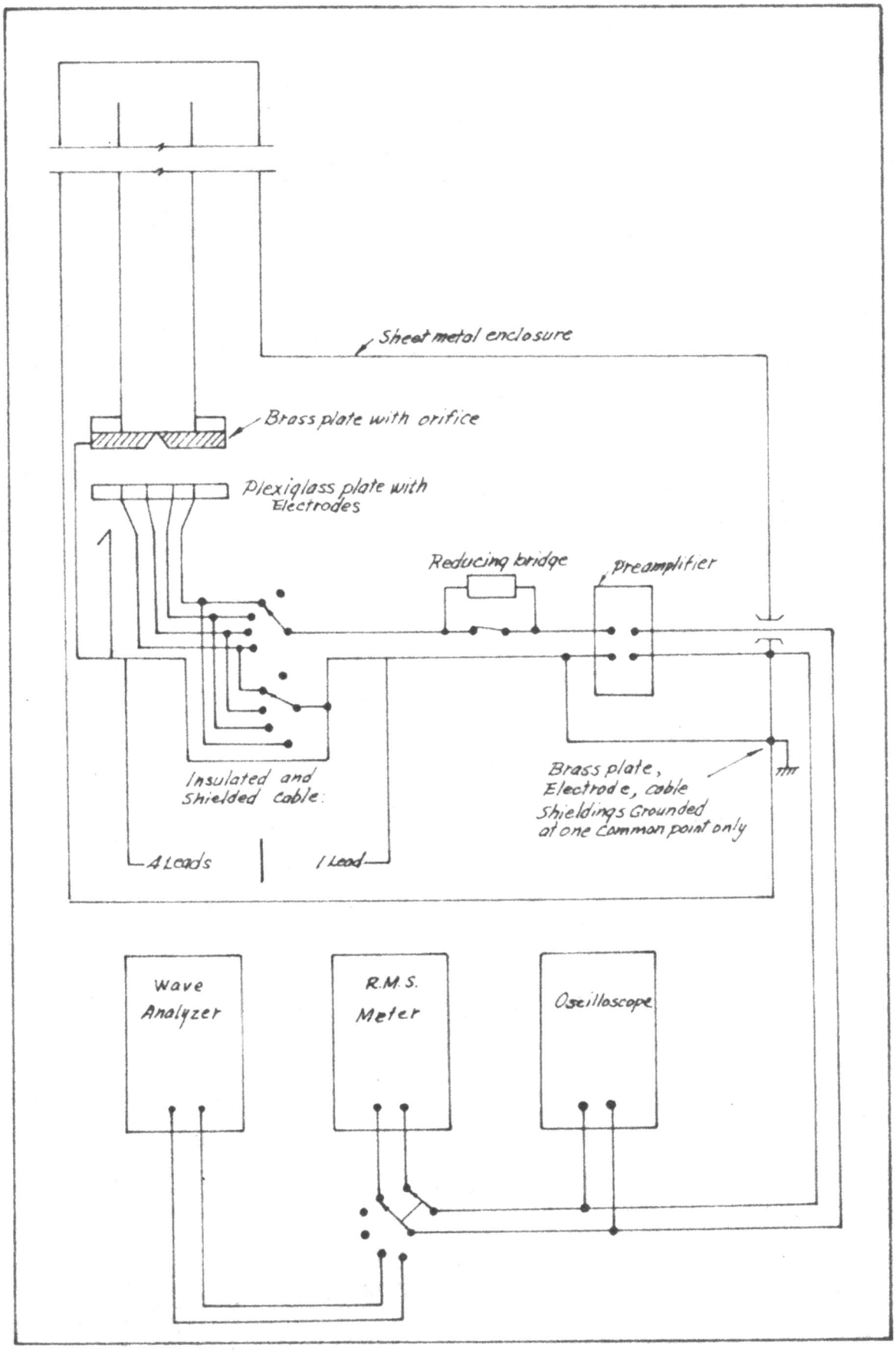

Fig. 3 Electrical System

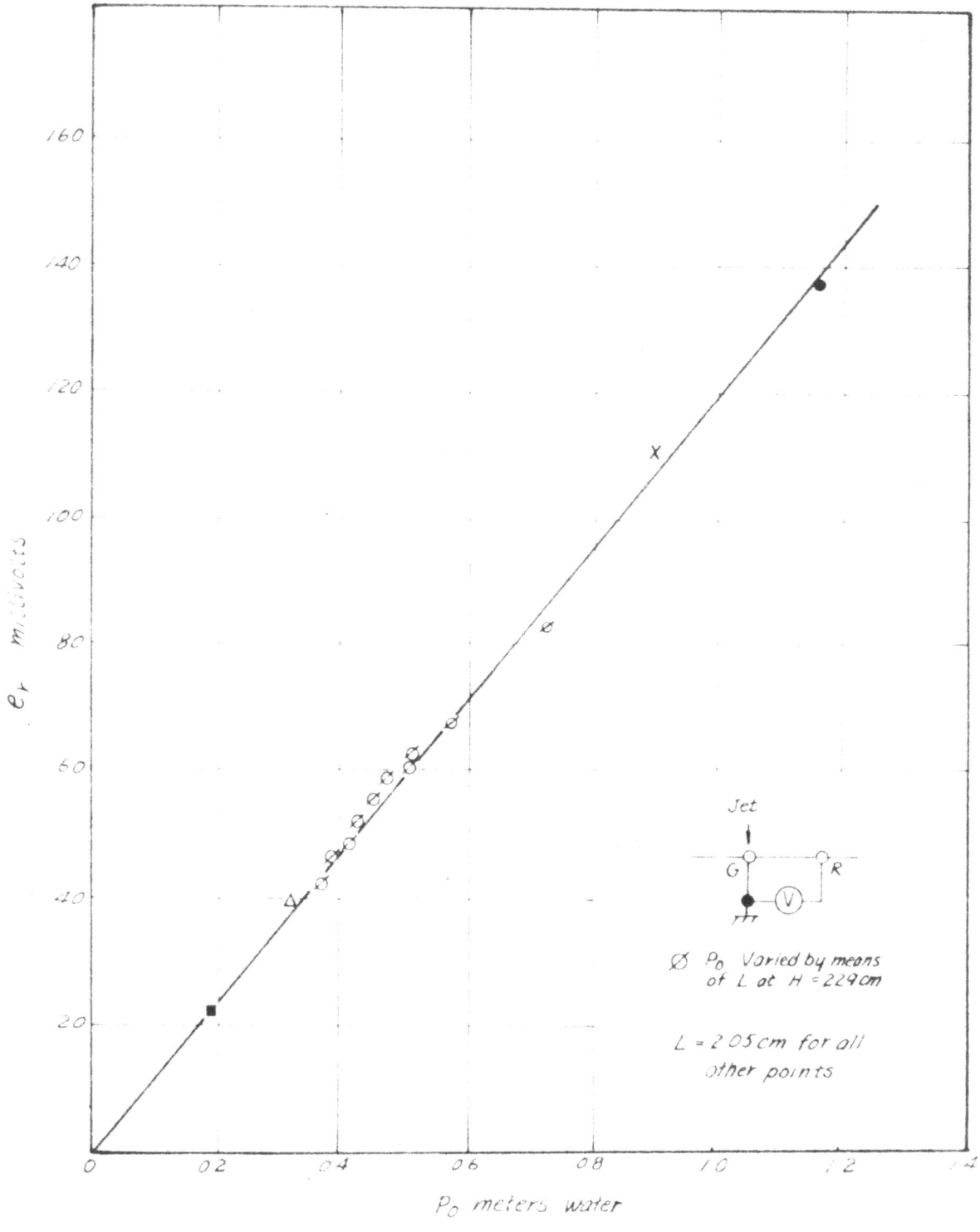

Fig. 4 Variation of Amplified Potential-Fluctuations with Stagnation Pressure

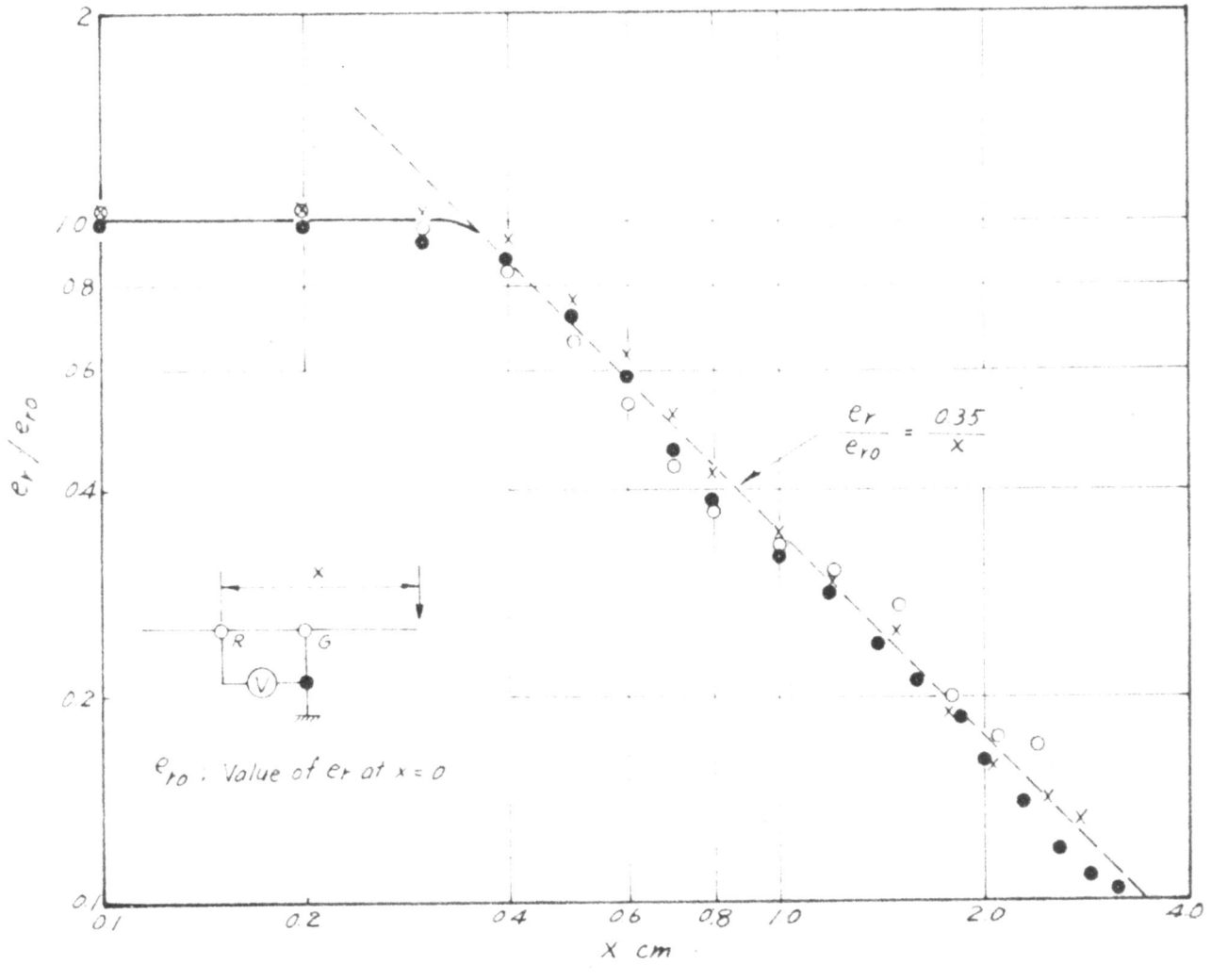

Fig. 5 Variation of Amplified Potential-Fluctuations at the wall as a Function of Distance from Stagnation Point

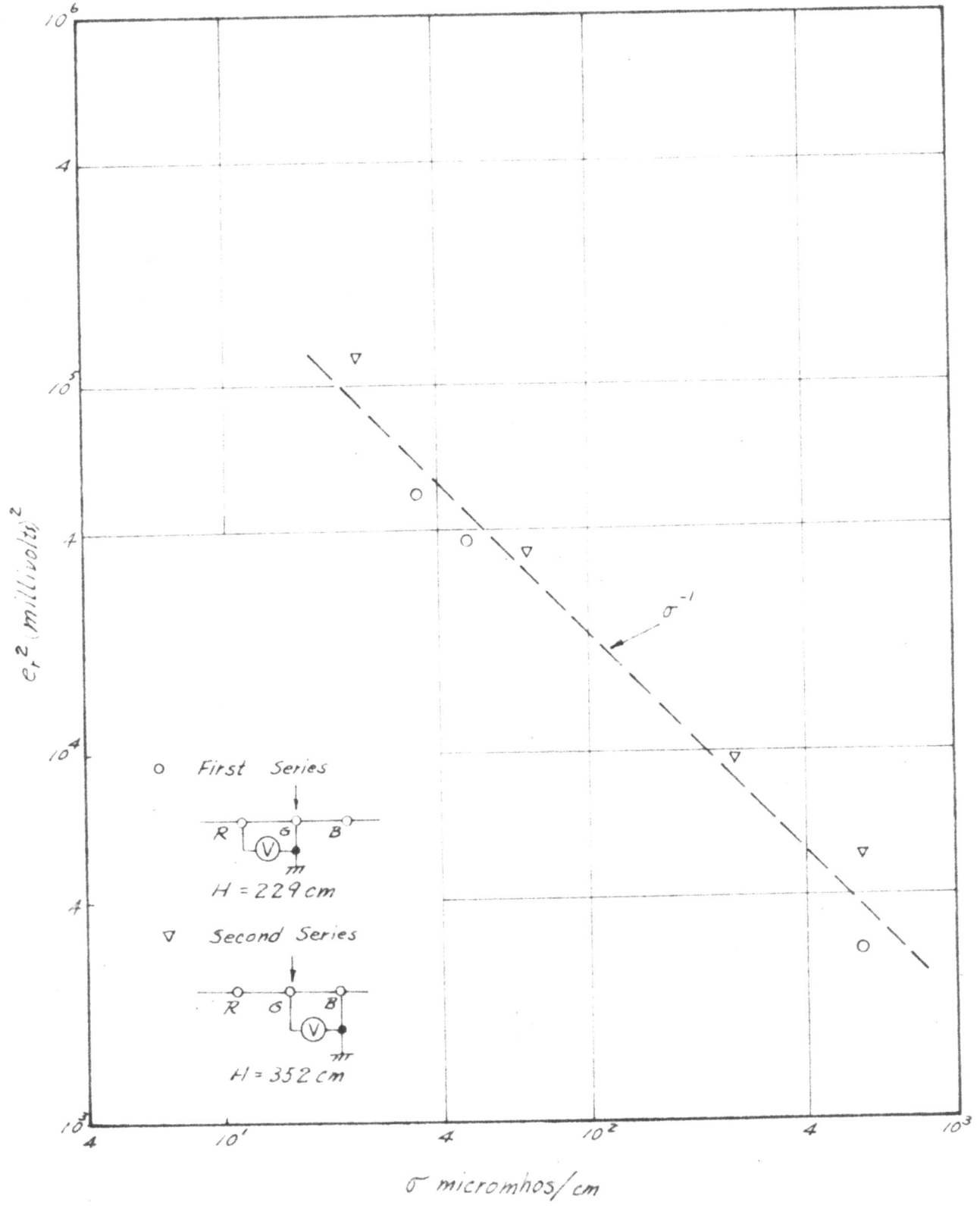

Fig. 6 Mean-Square of Amplified Wall Potential-Fluctuations with Electrical Conductivity of the Water

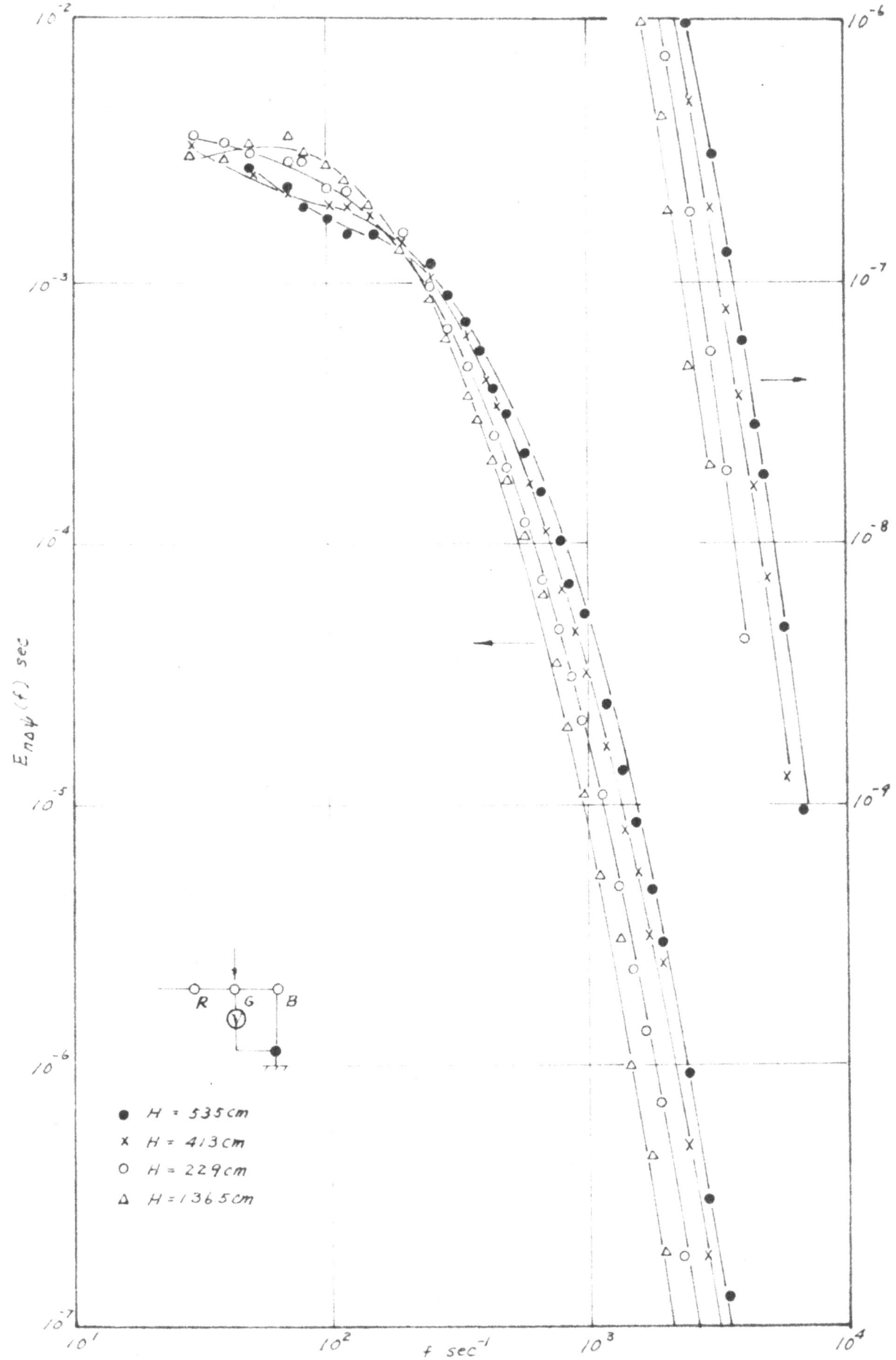

Fig 7 Frequency Spectrum at the Stagnation Point

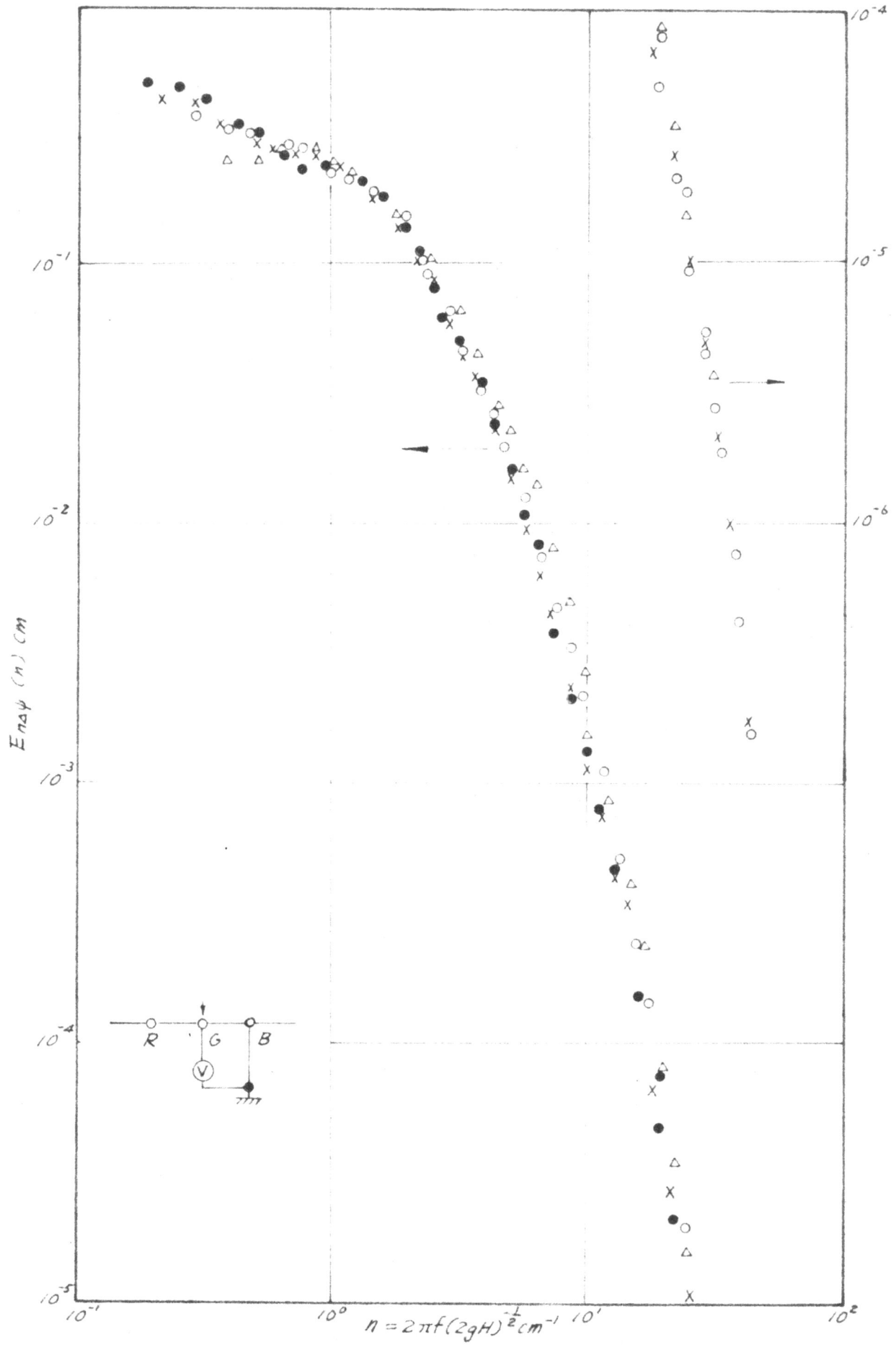

Fig. 8 Wave Number Spectrum at the Stagnation Point

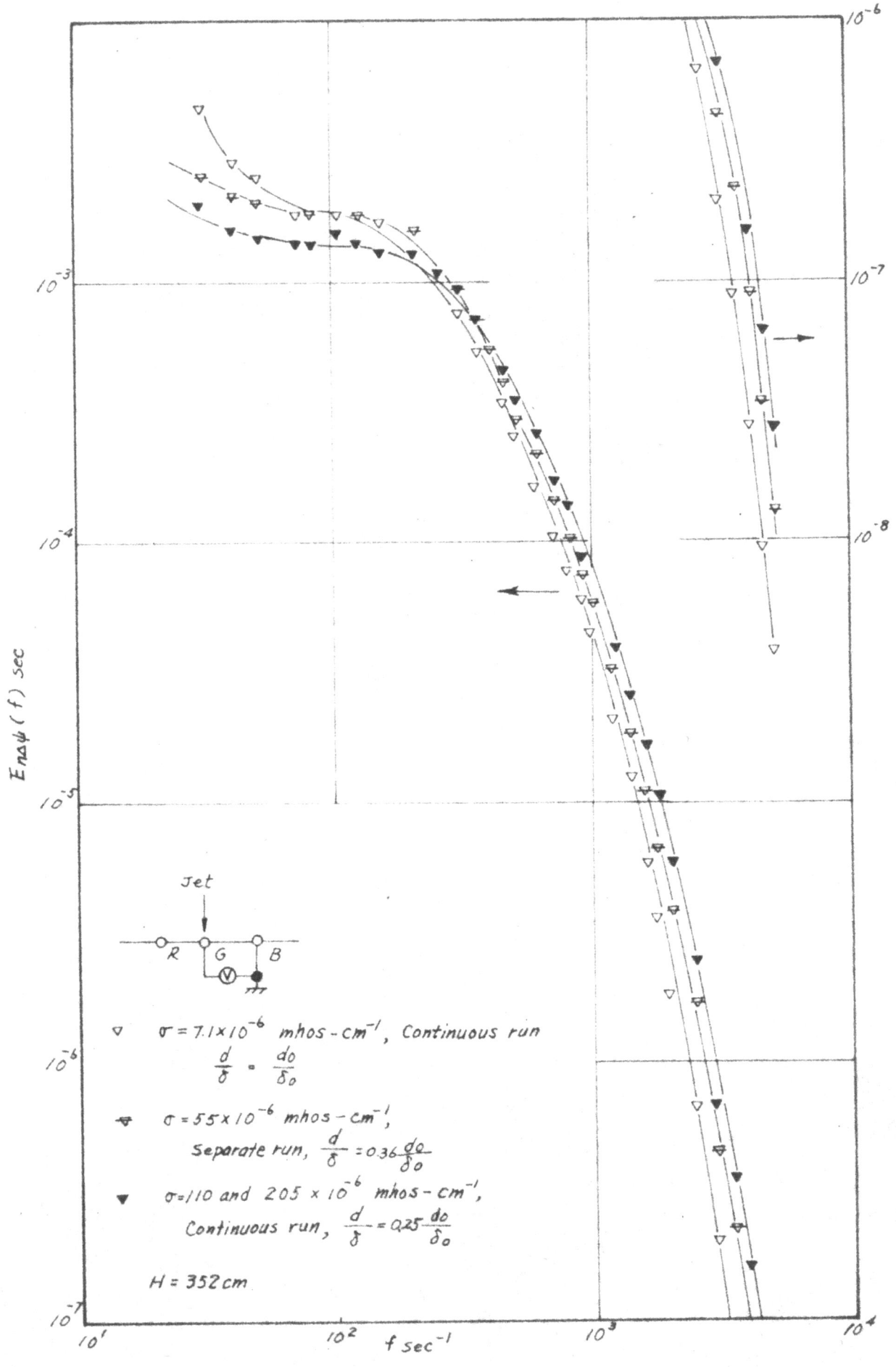

Fig 9 Variation of the Frequency Spectrum with the Electrical Conductivity of the Water

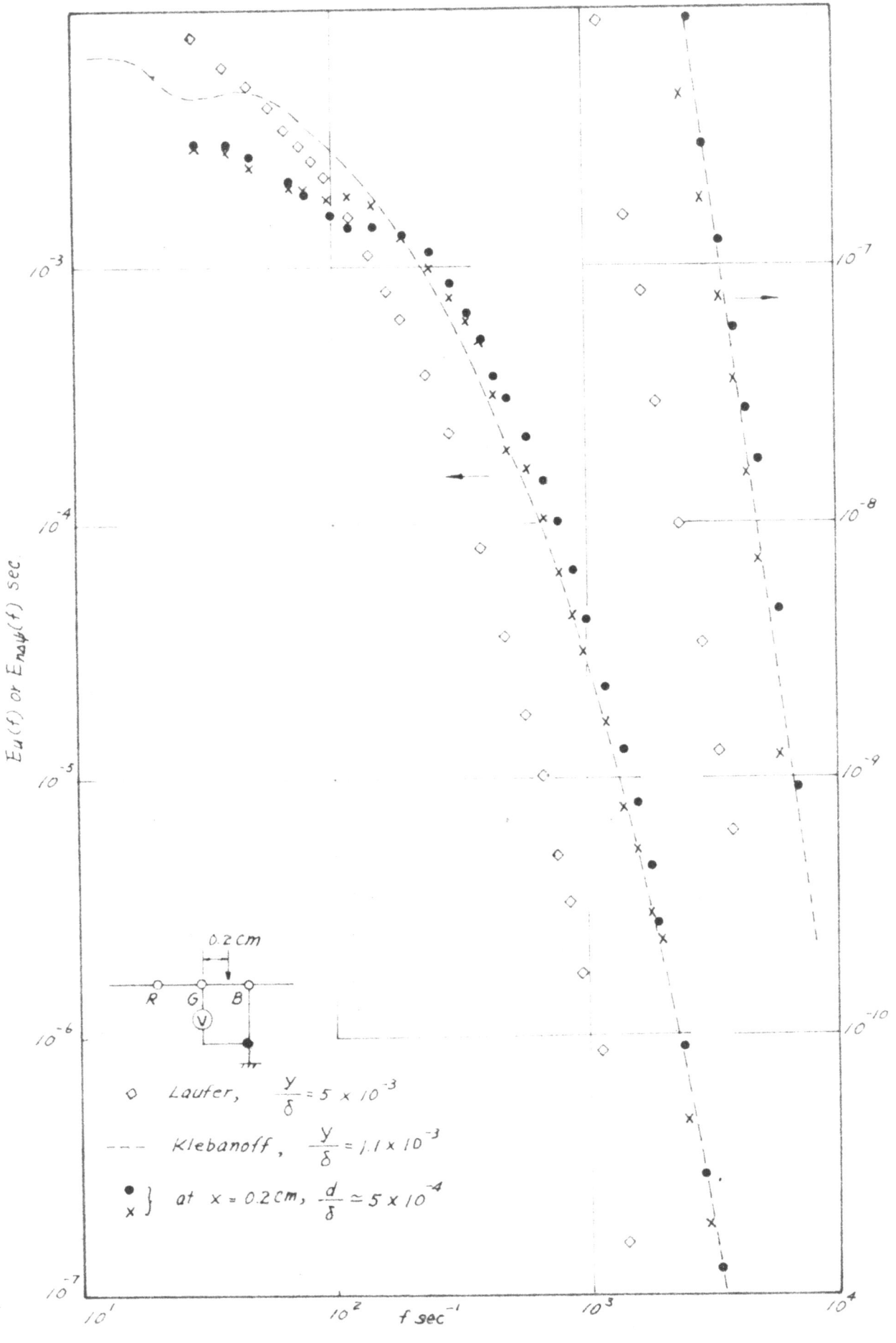

Fig. 10 Normalized Spectra for Potential and Velocity Fluctuations

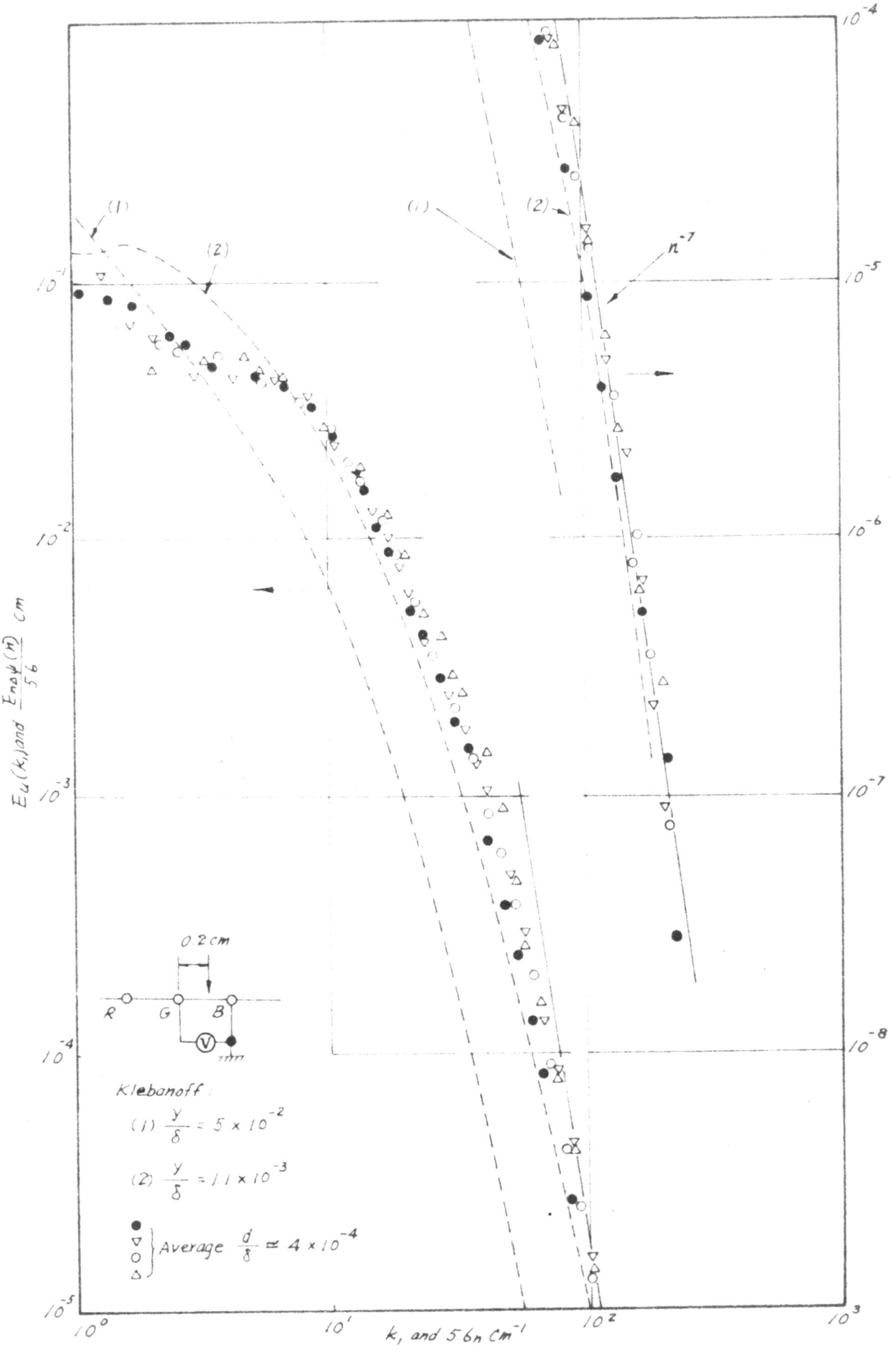

Fig. 11 Normalized Spectra for Potential and Velocity Fluctuations

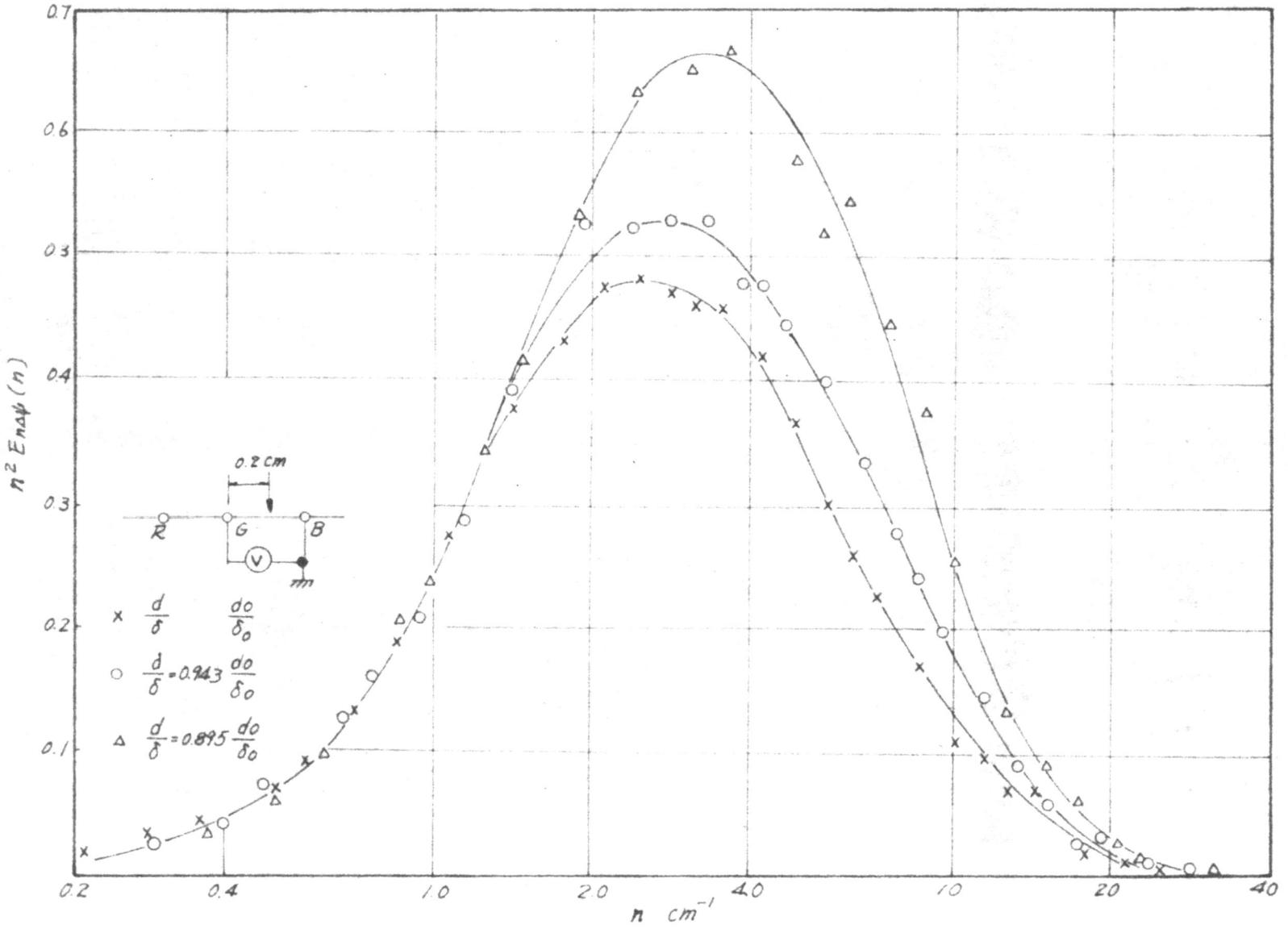

Fig. 12 Second Moment of Spectral Distribution